Environmental Science Advances

ROYAL SOCIETY OF CHEMISTRY

PAPER

View Article Online
View Journal | View Issue

Cite this: *Environ. Sci.: Adv.*, 2025, **4**, 1896

Assessing the impact of enhanced model resolution on heatwave prediction during June 2023

Sakshi Sharma, [b] Harvir Singh, [ac] Anumeha Dube, [a] Arun Chakraborty, *[b] M. N. Raghavendra Sreevathsa, [a] Raghavendra Ashrit [a] and V. S. Prasad [a]

Heatwaves are extreme weather events characterized by prolonged periods of unusually high temperatures, often leading to severe impacts on health, economy, and infrastructure. Global numerical weather prediction (NWP) models are useful for heatwave prediction, but they often underestimate the intensity due to their coarse resolution. To address this, experiments with high-resolution NWP models are required to better capture the intensity of heatwaves. In this study, we conducted an experiment using the National Centre for Medium Range Weather Forecasting (NCMRWF) Global Unified Model (NCUM-G) in two configurations: 12 km (Exp12) and 6 km (Exp06) resolutions, both initialized with identical conditions. To assess their performance, forecasts from the two versions were evaluated against the India Meteorological Department's (IMD) gridded observations using the mean error (ME) for the extreme heatwave over eastern India during 14–19 June 2023. The observed maximum temperature (T_{max}) during this event reached 42–46 °C, well above the climatological 32–36 °C, mainly due to a ridge over eastern India and delayed monsoon onset from cyclone Biparjoy. Results show that Exp06 provided superior accuracy at shorter lead times (Day 1 and Day 3), closely capturing the observed heatwave intensity, while Exp12 outperformed Exp06 at longer lead times (Day 5). Regional verification revealed that Exp06 forecasts aligned particularly well with observations over Uttar Pradesh and Bihar, while both models showed comparable performance over Jharkhand and Odisha. These findings highlight the trade-offs between the resolution and forecast range in global models and demonstrate that high-resolution experiments can substantially improve short-range predictions of extreme heatwaves in India.

Received 9th May 2025
Accepted 15th September 2025

DOI: 10.1039/d5va00122f

rsc.li/esadvances

Environmental significance

This study primarily focused on the short-term analysis of forecasts of the maximum temperature (T_{max}) over heatwave-prone regions during cyclone Biparjoy and assessed the forecast performance for different resolutions. It is observed that, on average, fine-resolution experiments are better capable of capturing the increase in T_{max}, particularly for longer lead times (Day 5) as compared to the coarse-resolution experiment, which has a tendency to underestimate T_{max} values in the study area. It is also evident that the fine-resolution experiment demonstrated reasonably superior performance for shorter lead times, as compared to the coarse-resolution experiment; the former had a lower mean error and the capability to forecast higher T_{max} values over the study area. As a result, the use of finer-resolution models can add value to the forecasts obtained for extreme events such as heatwaves, particularly for lead times up to Day 5. Conducting cross-validation with extended datasets will be a viable approach to ensure the robustness of the findings.

1. Introduction

In recent years, the world has seen a steady increase in the intensity and frequency of extreme weather events, such as heatwaves, cyclones, and heavy rainfall, with serious impacts on human lives and the economy.[1] Heatwaves, in particular, have become more frequent and intense since the 1950s, with projections indicating that much of Asia will experience more frequent temperature extremes in the future, leading to increased mortality and heat-related illnesses, especially among the elderly and urban poor.[2,3] Although the global trend shows an overall increase, the frequency and intensity of heatwaves exhibit significant regional variability.[4,5] Over India, the annual mean temperature has risen by about 0.85 °C between 1901 and 2015.[6] India is most susceptible to heatwaves from March to June, particularly in the northern, northwestern, eastern, and central regions.[7] Several studies have documented an increasing trend in heatwave occurrence across the country.[7–9] Ray *et al.*[10] reported a 24% rise in heatwave events during 2010–2019 compared to that during 2000–2009, accompanied by a 27% increase in mortality, making heatwaves the second most

[a]*National Centre for Medium-Range Weather Forecasting, Ministry of Earth Sciences, India. E-mail: arunc@coral.iitkgp.ac.in*

[b]*Centre for Ocean, River, Atmosphere and Land Sciences (CORAL), Indian Institute of Technology, Kharagpur, West Bengal, 721302, India*

[c]*Institute of Environmental and Sustainable Development, Banaras Hindu University, India*

disastrous weather-related hazard in India. Consistent with these findings, IMD datasets show a marked rise in the frequency and intensity of heatwaves in recent years.[11] Northern India, in particular, has experienced frequent heatwave episodes, with an annual average of five–six events.[12–16]

The definition of a heatwave varies across organizations and regions. According to the World Meteorological Organization (WMO, 2015), a heatwave is defined as a period of at least five consecutive days during which the daily T_{max} exceeds the climatological average by 5 °C or more. According to the India Meteorological Department (IMD), a heatwave is declared when the T_{max} of a station reaches at least 40 °C in the plains (37 °C in coastal regions and 30 °C in hilly areas) and departs from normal by 4.5–6.4 °C. A severe heatwave is declared when the deviation exceeds 6.4 °C or when the actual T_{max} reaches 45 °C (47 °C for severe heatwave), irrespective of the normal.[17] This criterion is also presented in Table 1. In addition, the Heat Index (HI), widely used by WMO, incorporates both temperature and relative humidity (RH) to reflect human-perceived heat stress.[18–20] As the presence of humidity in the environment diminishes the body's ability to cool itself, the high temperature becomes even more intolerable with an increase in RH. During May 2010, a severe heatwave over Ahmedabad, Gujarat, led to extreme heat stress conditions and caused a 41% rise in all-cause mortality.[21] Similarly, during 14–19 June 2023, the states of Uttar Pradesh, Bihar, Jharkhand, and Odisha in eastern and central India experienced a severe heatwave that resulted in numerous deaths and hospitalizations. The heatwave began on 14th June and persisted until 19th June, with T_{max} exceeding 42 °C over eastern Uttar Pradesh on 16 June, which resulted in several heat-related casualties. The event intensified due to large-scale circulation features, particularly tropical cyclone 'Biparjoy', which brought heavy rainfall to Gujarat and Rajasthan (western India) and consequently delayed the advance of the southwest monsoon into central and eastern India. This delay, combined with persistently high T_{max} and RH and the absence of rainfall, created conditions that sustained and exacerbated the extreme heatwave over eastern India. Therefore, obtaining timely and accurate forecasts of such extreme events is crucial for effective planning and disaster mitigation.

Numerical Weather Prediction (NWP) models have proven useful for predicting heatwaves in India and are therefore an effective tool for providing timely forecasts and supporting disaster mitigation.[12] Advances in computing power and modeling techniques have enabled these systems to generate more accurate maximum temperature (T_{max}) forecasts, even over tropical regions.[22] Several studies have shown that NWP models can reasonably reproduce the increases in T_{max} associated with heatwave conditions over India.[23] In particular, high-resolution model simulations, combined with high-frequency output on high-performance computing platforms, exhibit an improved ability to predict extreme temperatures at longer lead times.[24] However, a key limitation remains that global models, due to their relatively coarse resolution, often underestimate the intensity and local variability of extreme heatwave events.[8,25]

The National Centre for Medium Range Weather Forecasting (NCMRWF) Unified Model has been used operationally in India since 2012.[26–28] Its global configuration (NCUM-G) runs at a horizontal resolution of 12 km (Exp12), with 70 vertical levels. Recently, NCMRWF developed a higher-resolution version of the NCUM-G, increasing the horizontal resolution to 6 km (Exp06) while keeping the model's physics unchanged. This provided an opportunity to evaluate how increased resolution influences the forecasting of extreme weather events. In this study, we tried to evaluate the predictive capabilities of both configurations to assess the influence of resolution on T_{max} forecasts associated with heatwaves. Specifically, we examined the extreme heatwave event of 14–19 June 2023 over eastern and central India, Odisha, to understand the benefits and limitations of high resolutions for forecasting such high-impact events.

The main aims of this study are: (a) to evaluate the impact of model resolution on heatwave forecasts by comparing two global configurations of the NCUM-G model, Exp12 and Exp06, which are initialized with identical physics and initial conditions, thereby isolating the effect of horizontal resolution on predicting heatwave intensity; (b) to analyze the synoptic setting of the June 2023 heatwave over eastern India, particularly how the delayed monsoon onset due to Cyclone Biparjoy, combined with a persistent ridge over the region, contributed to the intensification of the event. The manuscript is divided as follows: Section 2 provides information about the study area, dataset used, and model description. The results are presented in Section 3. The overall conclusions drawn from the study are listed in Section 4.

2. Study area, data, model, and methodology

2.1 Study area

The geographical locations of the study regions are shown in Fig. 1. The region affected by the heatwave during 14–19 June 2023 is presented within the black box. The climatological T_{max} values for this region range between 36 °C and 38 °C during March to June.

2.1.1 Climatology over the study area during June. The June climatology (1979–2022) over India shows (Fig. 2) a distinct pre-monsoon heating pattern, with the T_{max} exceeding 40 °C

Table 1 IMD heatwave criteria (https://internal.imd.gov.in/section/nhac/dynamic/FAQ_heat_wave.pdf)

Based on the departure from normal	Heatwave (HW): departure from normal is 4.5 °C–6.4 °C Severe HW: departure from normal is > 6.4 °C
Based on the actual T_{max}	HW: when the actual T_{max} is 45 °C Severe HW: when the actual T_{max} is 47 °C

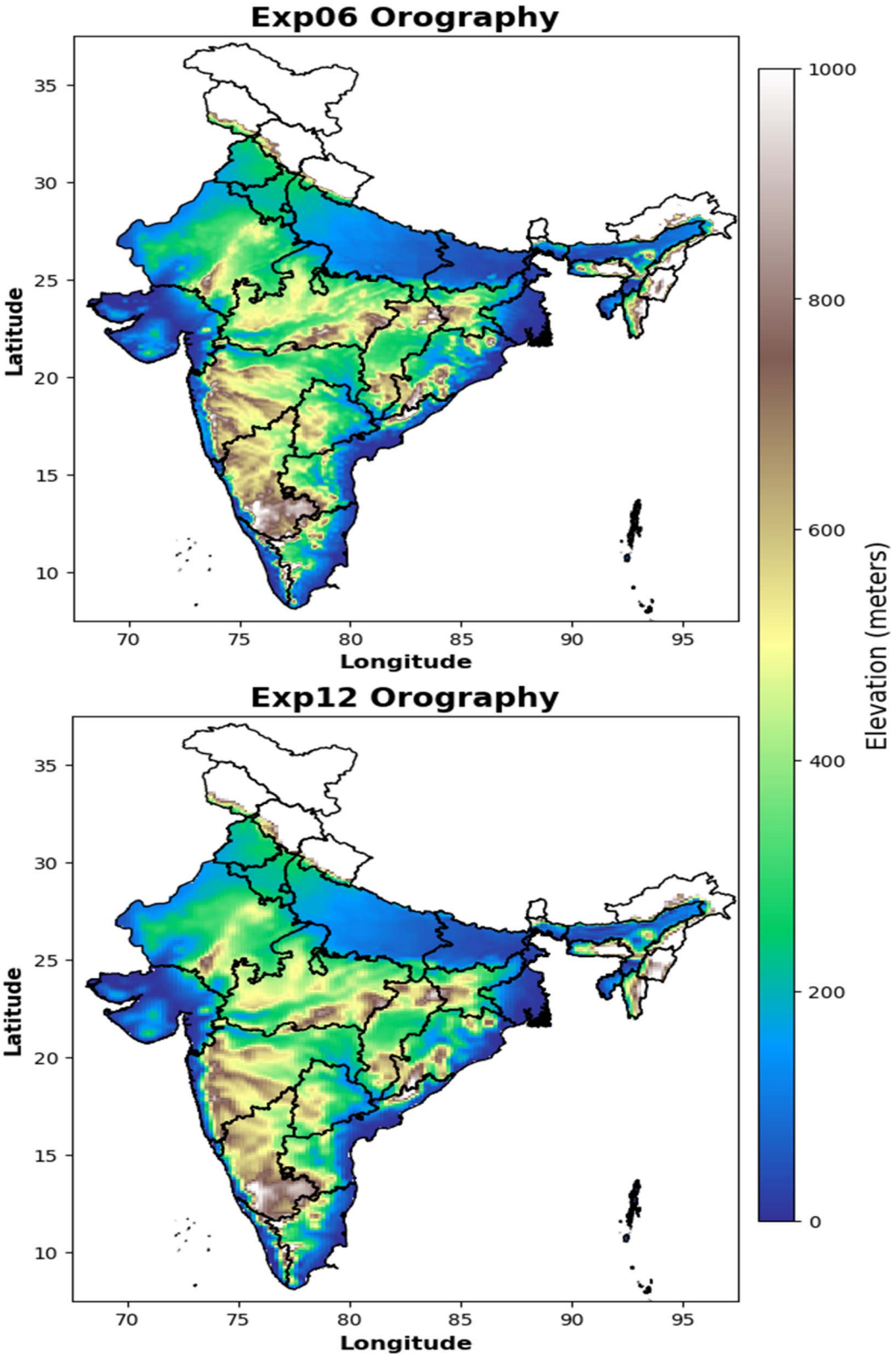

Fig. 1 Geographical locations with background orography (m) for Exp12 and Exp06 in India, highlighting the state boundaries.

over northwestern and central India, while relatively cooler conditions (<32 °C) prevail over the southern peninsula and along the coasts. RH exhibits an opposite gradient, remaining low (50–60%) across northwest and north-central India but higher (>70%) in eastern and southern parts, influenced by the advancing monsoon flow. Surface winds at 10 m (W10)

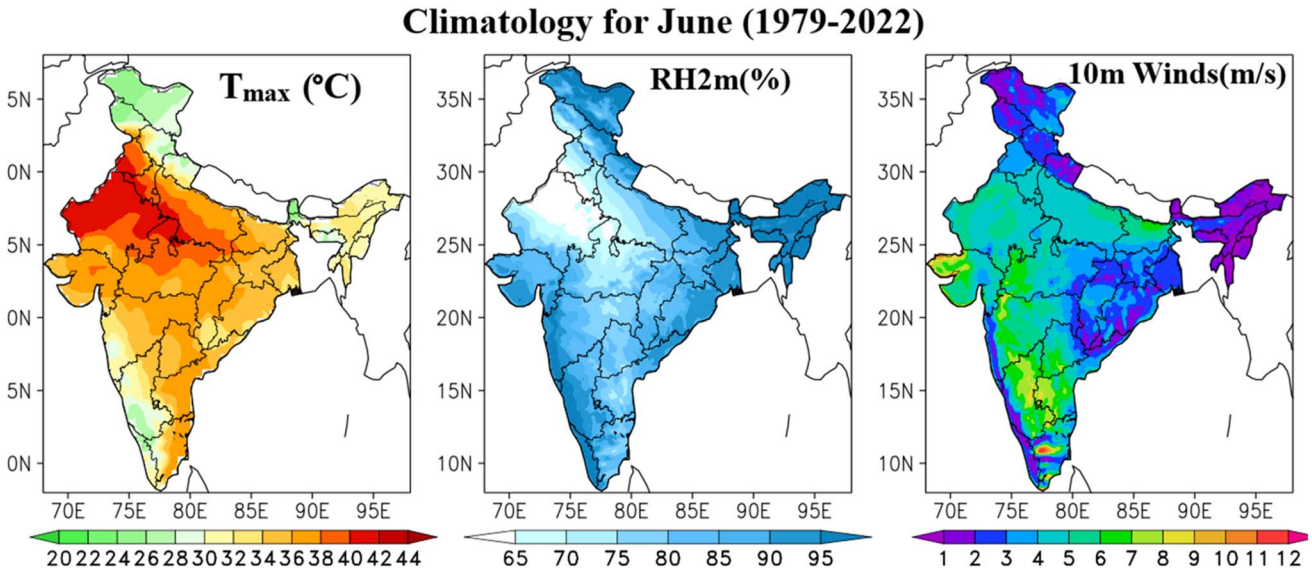

Fig. 2 Climatology (1979–2022) of T_{max}, RH2m (%) and W10 over the Indian land region. T_{max} climatology is obtained from IMD gridded data, whereas RH2m and W10 are obtained from IMDAA reanalysis data.

highlight the strengthening southwesterlies over peninsular and northeastern India (>5 m s^{-1}), while much of northwest and central India remains under weaker flow (<3 m s^{-1}), allowing heat to persist. In particular, the states of Uttar Pradesh, Bihar, and Odisha display climatological features that make them particularly prone to heatwave conditions. Uttar Pradesh and Bihar typically record T_{max} in the range of 36–42 °C with low RH (<55%), reflecting intense pre-monsoon heating under stagnant conditions. In contrast, Odisha generally experiences slightly lower T_{max} (32–36 °C) but with higher RH (60–70%), reflecting early monsoon moisture inflow from the Bay of Bengal. However, the surface winds over these regions remain weak (<3 m s^{-1}), limiting ventilation and thereby compounding thermal stress. This climatological combination—hot and dry in UP/Bihar, hot and humid in Odisha—creates a background highly conducive to severe heatwave development, especially when monsoon onset is delayed. The T_{max} climatology is based on IMD gridded observations,[13] while RH and wind speed climatologies are obtained from the IMDAA regional reanalysis.[29]

2.2 IMD observed t_{max} data

The observed 2 m temperatures (T_{max} and T_{min}) are a gridded dataset over the Indian land region (7.5°N–37.5°N, 67.5°E–97.5°E), which is developed by the IMD and has a resolution of 0.5° × 0.5° (**https://www.imdpune.gov.in/Seasons/Temperature/max/Max_Download.html**). These datasets are archived at the National Data Centre (NDC) of the IMD in Pune and assessed through the data processing procedure based on Srivastava *et al.*[13] We have used these daily gridded T_{max} data[13,30] for heatwave verification with model experimental forecasts.

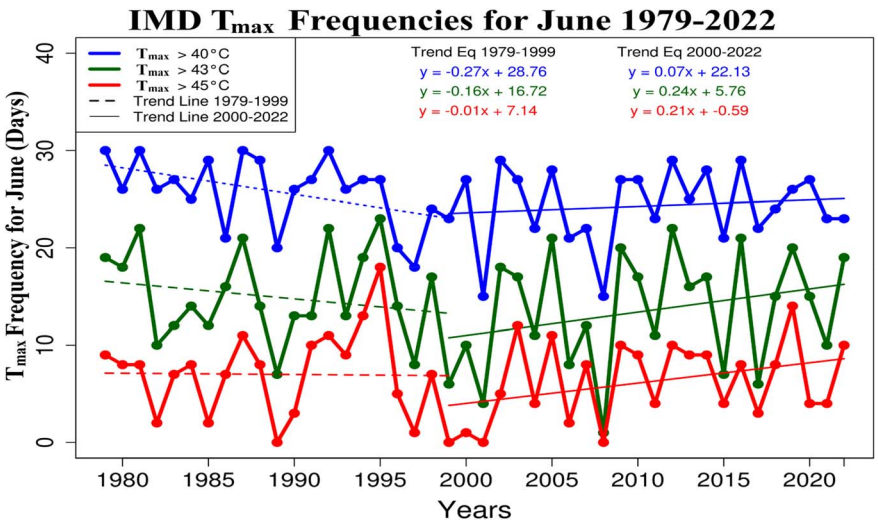

Fig. 3 Trend analysis of the different T_{max} frequencies for June from 1979 to 2022.

2.2.1 Climatology of t_{max} over India. To examine the changes in the intensity and frequency of heatwaves over India, a trend analysis of T_{max} thresholds (>40 °C, >43 °C, and >45 °C) was carried out for the March–June season during the 1979–2022 period (Fig. 3). The results clearly indicate an increasing number of hot days over the years. It is also observed that during the 1970–1999 period, the trend is negative despite the general climate warming. In the past decade, several years recorded more than 80 days with T_{max} > 40 °C and over 50 days with T_{max} > 43 °C. Notably, the year 2010 alone registered nearly 30 days above 45 °C, highlighting the severity of extreme heat events.

The decadal changes in frequency of these extreme-temperature days are summarized in Table 2, covering five decades from 1980 to 2020. During 1980–1989, there was a modest increase in the number of hot days: 4 days above 40 °C, a larger rise of 11 days above 43 °C, and a substantial increase of 20 days above 45 °C. However, the following decade (1990–1999) showed a sharp decline, with decreases of 21, 16, and 15 days for the three thresholds, respectively. The trend reversed in 2000–2009, when the number of hot days increased again by 11 (≥40 °C), 12 (≥43 °C), and 15 (≥45 °C). The maximum change is seen in the last decade (2010–2020), where there were 64 days with T_{max} > 40 °C, 53 days with T_{max} > 43 °C, and 46 days with T_{max} > 45 °C.

Table 2 Decadal change in the frequency of T_{max} days for June from 1980 to 2022

Decade	Decadal change in the number of days with $T_{max} \geq 40$ °C	Decadal change in the number of days with $T_{max} \geq 43$ °C	Decadal change in the number of days with $T_{max} \geq 45$ °C
1980–1989	44	44	14
1990–1999	−15	2	16
2000–2009	−15	−26	−24
2010–2020	21	30	25

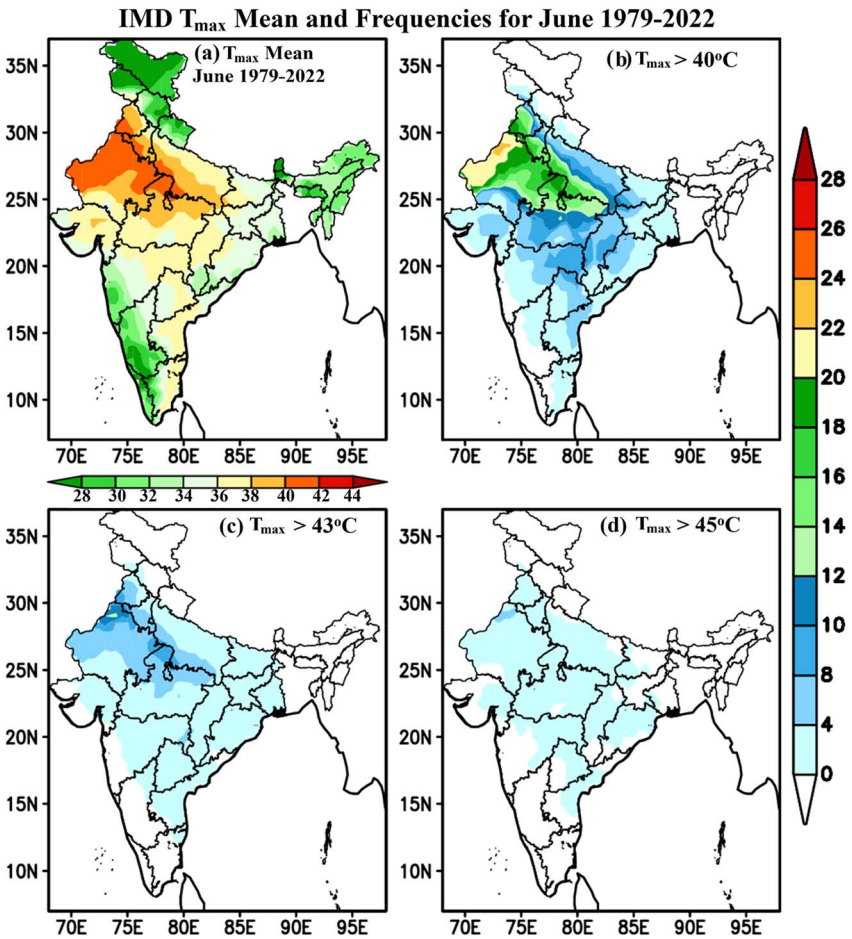

Fig. 4 (a) T_{max} climatology as well as T_{max} frequencies, (b) T_{max} > 40 °C, (c) T_{max} > 43 °C, and (d) T_{max} > 45 °C, for the month of June from 1979 to 2022.

In addition to the temporal trends, the spatial distributions of the T_{max} climatology and frequency during June for the 1979–2022 period are shown in Fig. 4. The mean June T_{max} (Fig. 4a) clearly identifies northwest and adjoining central India as the climatological core heat regions, with Rajasthan, Haryana, Punjab, Uttar Pradesh, and western Madhya Pradesh exhibiting mean values frequently exceeding 36–38 °C, and localized pockets surpassing 40 °C. In contrast, southern and northeastern India remain relatively cooler, with climatological means below 32 °C. The frequency distributions provide a more nuanced perspective on the prevalence of extreme heat. Days with T_{max} > 40 °C (Fig. 4b) occur with striking regularity over northwest and central India, where 15–20 days in June are typical. This implies that, in many locations within Rajasthan and adjoining states, nearly two-thirds of June days consistently cross the 40 °C threshold. The occurrence of days with T_{max} > 43 °C (Fig. 4c) is more restricted, generally limited to 5–10 days in June across Rajasthan, Haryana, and western Uttar Pradesh, while eastern and southern India record only isolated events. The most extreme category, T_{max} > 45 °C (Fig. 4d), though rare, still occurs climatologically up to 2–4 days in June in western Rajasthan and adjoining pockets of northwest India, underscoring the severity of heat stress in this region. This section shows that northwestern India is the climatological core of heat extremes, while states such as Uttar Pradesh, Bihar, Jharkhand, and Odisha also experience frequent hot days during June, making them vulnerable to recurrent heatwave episodes.

2.2.2 T_{max} during June 2023. The June 2023 T_{max} distribution (Fig. 5) shows a departure from the long-term climatology (Fig. 4). Unlike the climatological pattern, where the highest frequencies of extreme heat are confined to northwestern India, June 2023 exhibited an eastward shift of the heat core. The mean June T_{max} (Fig. 5a) remained anomalously high across eastern Uttar Pradesh, Bihar, Jharkhand, and Odisha, with large areas recording averages of 36–38 °C, which climatologically are expected only over northwest India. Frequencies of extreme thresholds also indicate this anomalous behavior. The number of days with T_{max} > 40 °C (Fig. 5b) exceeded 10–14 across much of eastern and central India, including Bihar, Jharkhand, and Odisha, compared to the climatological expectation of fewer than 2–4 days. Similarly, occurrences of T_{max} > 43 °C (Fig. 5c), typically restricted to Rajasthan and Haryana based on the climatology, are also seen over parts of eastern Madhya Pradesh, Jharkhand, and adjoining Odisha, where up to 4–6 days were recorded. Even the most severe category, T_{max} > 45 °C (Fig. 5d), showed isolated instances in central and eastern India where such extremes are unusual in this month. This comparison demonstrates that heatwave activity was intense during June 2023 and also shifted from northwestern India to the eastern states. This change in the geographical location of the temperature maxima can be attributed to the combined influence of delayed monsoon progression and anomalous synoptic forcing associated with Cyclone Biparjoy.

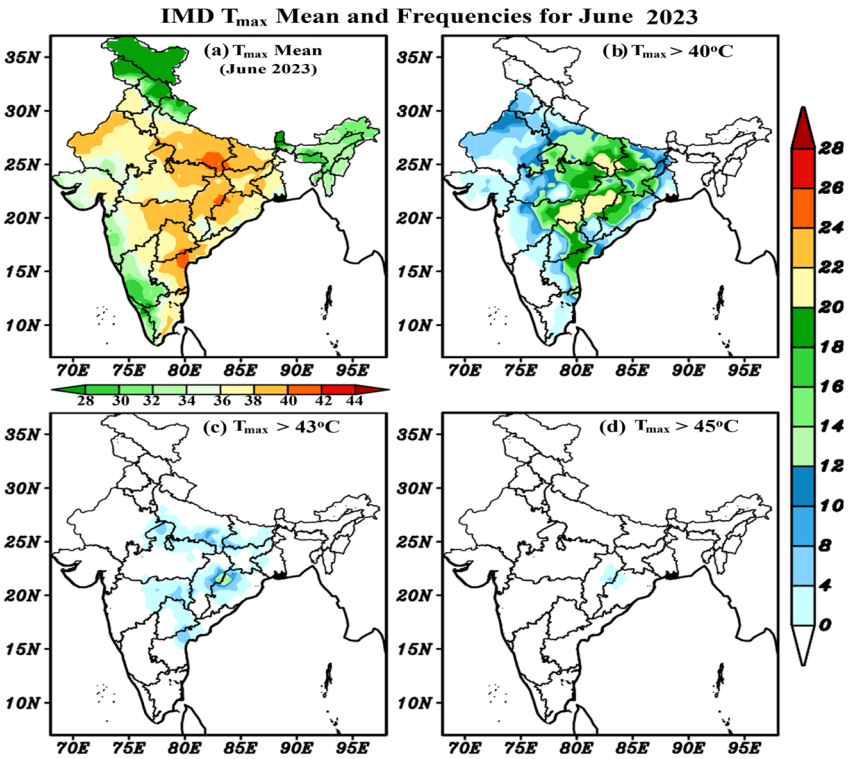

Fig. 5 (a) T_{max} climatology as well as T_{max} frequencies, (b) T_{max} > 40 °C, (c) T_{max} > 43 °C, and (d) T_{max} > 45 °C, for the month of June for the year 2023.

2.3 NCMRWF unified model (NCUM-G, Exp12)

The NCUM-G model has been operational at NCMRWF since 2012 (ref. 26–28) and is based on the unified model (UM11.2) developed under the "UM Partnership" and implemented within the UK Met Office's "Operational Global Suite" (PS43). The NCUM framework is updated periodically to incorporate advances in dynamics, physics, and data assimilation. The current operational NCUM-G runs at a horizontal resolution of ~12 km (N1024) with 70 vertical levels and a 5-minute time step, and it provides 10-day forecasts initialized at 00 and 12 UTC each day. The model is coupled with a hybrid four-dimensional variational (4D-Var) data-assimilation system[31] that combines conventional, satellite radiance, and aircraft observations, thereby ensuring improved initial conditions for forecasts.[28] Continuous upgrades in observation handling, assimilation techniques, and physical parameterizations have significantly enhanced its capability to represent the monsoon circulation and high-impact weather systems over India and adjoining regions.

2.4 NCUM-G (Exp06)

NCMRWF has recently undertaken the in-house development of a high-resolution (6 km) version of the NCUM-G model, aimed at improving the representation of high-impact weather events, such as heatwaves. The high-resolution experimental suite (Exp06) generates forecasts up to 5 days from the 00 UTC initial conditions, employing the Global Atmosphere (GA) 7.0 physics configuration,[32] identical to that used in the operational 12 km configuration (Exp12). The horizontal grid employs a land–sea mask derived consistently from the model orography, while the model integration is advanced with a 3.0-minute time step to ensure numerical stability at this finer resolution. For this study, forecasts from the two versions of NCUM-G were obtained (summarized in Table 3):

Both configurations are initialized from identical Hybrid 4D-Var data assimilation[28] analyses, ensuring consistent initial conditions. The model physics, dynamical core, and explicit physical parameterizations are kept unchanged between the two experiments, allowing the study to isolate the impact of horizontal resolution on forecasts of extreme heatwave conditions.

2.5 Verification methodology

The verification of forecasts from the above two versions of NCUM-G was carried out using the gridded observations of daily T_{max} from the IMD, which serves as the reference dataset. To assess model performance, multiple approaches were adopted:

- The Mean Error (ME) was calculated at grid points over the affected states (Uttar Pradesh, Bihar, Jharkhand, and Odisha), providing a measure of systematic bias in the forecasts relative to the observations.
- Climatological departures: forecast and observed anomalies were derived relative to the IMD June climatology (1981–2010 base period). These departures enable the evaluation of the models' ability to correctly capture the extremeness of the June 2023 heatwave beyond the seasonal background state.
- Time series analysis: spatially averaged T_{max} values were extracted over the study region to generate time series for both model forecasts and observations. This allowed the assessment of how well each model captured the temporal evolution of the heatwave, including onset, peak intensity, and decay.
- Synoptic diagnostics: to complement statistical verification, large-scale circulation features were analyzed, including geopotential height fields, wind patterns, and monsoon progression. Special focus was given to the role of tropical cyclone Biparjoy, which delayed monsoon onset and enhanced subsidence over eastern India, thereby prolonging the heatwave conditions.
- Statistical significance testing: to assess whether the differences in forecast skill between Exp12 and Exp06 are robust, a paired Student's *t*-test was applied to the ME values. The *t*-test evaluates whether the average difference between the two model forecasts is statistically distinguishable from zero, *i.e.*, whether the apparent improvement in Exp06 over Exp12 is due to systematic performance or could have arisen randomly. In this study, significance levels at 95% ($p < 0.05$) and 90% ($p < 0.10$) were considered, with the latter included given the limited sample size typical of short-duration extreme events.

By combining grid-wise error statistics, climatological departures, time series comparisons, and synoptic diagnostics, the verification framework provides a comprehensive evaluation of the model's performance. This multi-dimensional approach quantifies forecast skill, captures the temporal and spatial evolution of the heatwave, and elucidates the physical drivers underpinning the event, thereby offering a stronger assessment of the role of model resolution in heatwave prediction.

3. Results and discussions

3.1 Comparison of T_{max} based on climatology and observational data

Fig. 6(a and b) illustrate the spatial evolution of the daily maximum temperature (T_{max}) across India during 12–19 June 2023, compared against the corresponding long-term

Table 3 Salient features of the Exp12 and Exp06 versions of NCUM-G

Feature name	Exp12	Exp06
Model	Unified model version 11.2	Unified model version 10.8
Model time step	5 Minutes	3 Minutes
Long forecast length	10-day forecast for 00 UTC and 12 UTC	5-day forecast for 00 UTC
Initial condition	Hybrid 4D-Var data assimilation	Hybrid 4D-Var DA
Grid size	N1024 with 70 vertical levels	N2048 with 70 vertical levels

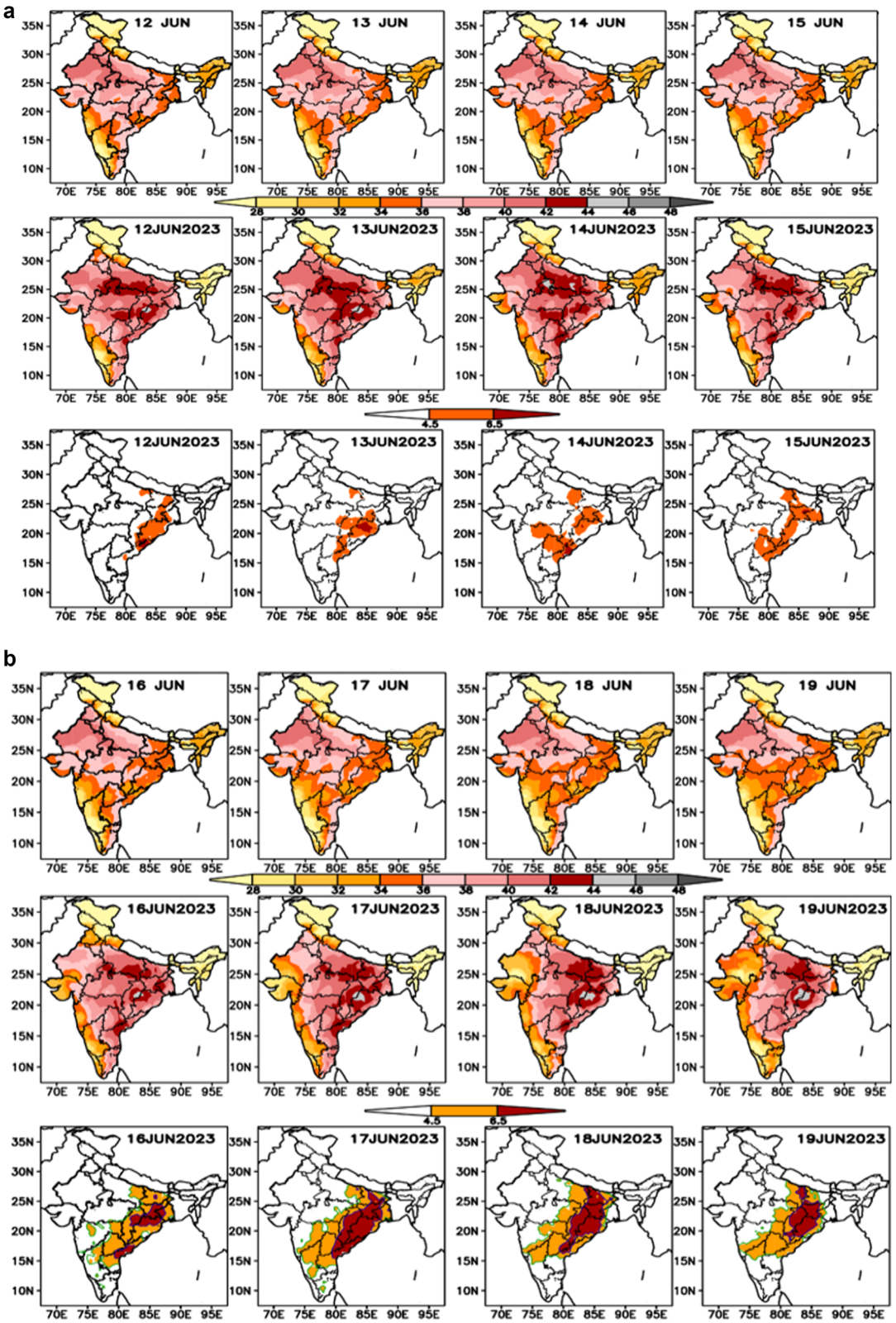

Fig. 6 (a)Comparison of the IMD daily T_{max} climatological values for June 12–15 (upper panel), daily T_{max} for 12–15 June 2023 (middle panel), and daily T_{max} departure from the climatological expectations (bottom panel). (b) Comparison of IMD daily T_{max} climatological values for June 16–19 (upper panel), daily T_{max} for 16–19 June 2023 (middle panel), and daily T_{max} departure from the climatological expectations (bottom panel).

climatology (1979–2022), along with departures from the climatological mean. This period coincided with a pronounced pre-monsoon heatwave over eastern and central India, which persisted for more than a week.

During 12–15 June (Fig. 6a), climatological T_{max} over eastern Uttar Pradesh, Bihar, Jharkhand, and adjoining regions over eastern India typically ranges from 34 °C to 40 °C. However, the observed T_{max} values in June 2023 were substantially higher, exceeding 42 °C across wide spatial domains and locally reaching 45–46 °C. The anomaly fields presented in the bottom row of the figure clearly show widespread positive departures exceeding +4.5 °C, with localized extreme anomalies surpassing +6.5 °C, which, according to the IMD criteria (Table 1), corresponds to a severe heatwave condition. The strongest anomalies were concentrated over Bihar, eastern Uttar Pradesh, and Jharkhand, while Odisha experienced isolated severe heatwave episodes, particularly on 13 June when the observed T_{max} approached 46 °C. For the 16–19 June period (Fig. 6b), the climatological T_{max} in eastern India decreased to 32–36 °C, which was attributed to the onset of the southwest monsoon, which moderates land surface heating through increased cloud cover and moisture advection. In contrast, the observed T_{max} during June 2023 remained anomalously high, ranging from 42 °C to 44 °C, with isolated hotspots exceeding 46 °C, particularly over Odisha and adjoining regions. The persistence of anomalies above +4.5 °C and in several cases above +6.5 °C shows the unusual nature of this heatwave event, both in terms of intensity and duration.

The departure plots show that large areas of eastern India experienced sustained extreme heat (for almost 7 to 8 days), indicating that the heatwave was widespread and persistent. This suggests that the event was not isolated but regionally organized, likely influenced by large-scale atmospheric circulation anomalies suppressing convection and delaying monsoon onset. The persistence of extreme heat during a climatological transition phase (pre-monsoon to monsoon) makes this episode particularly significant.

Overall, the analysis of Fig. 6a and b reveals three key scientific insights:

(a) Anomalous intensity – the T_{max} values exceeded the climatological ranges by 4–8 °C, with extremes above 45 °C observed in multiple states.

(b) Persistence – the heatwave persisted for at least eight consecutive days, satisfying both the intensity and duration criteria of the IMD's operational heatwave definition.

(c) Climatological context – the event occurred during a period when climatology suggests a cooling trend due to monsoon onset, thereby highlighting the severity of the anomaly.

This prolonged and spatially extensive heatwave event thus represents a clear departure from climatological expectations and provides a strong case for further investigation of the role of

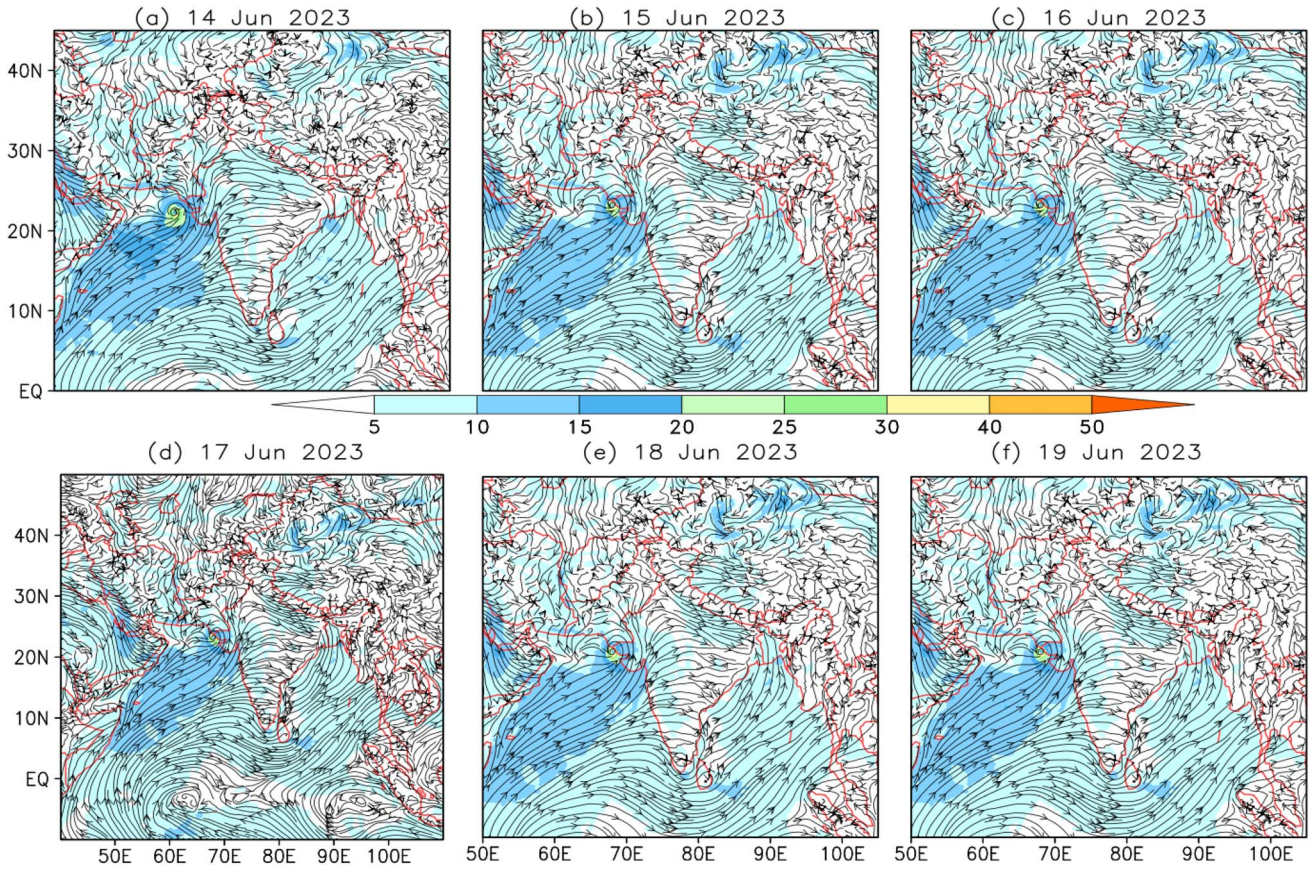

Fig. 7 Exp12 analysis W10 during 14 to 19 June 2023 with the magnitude displayed in colour shading.

large-scale circulation, land–atmosphere feedbacks, and delayed monsoon dynamics in amplifying regional extremes.

3.2 Synoptic features during 12 to 19 June 2023

The occurrence and persistence of heatwaves are strongly modulated by large-scale synoptic conditions. To investigate this, a detailed analysis of wind circulation, relative humidity, and surface temperature from the Exp12 analysis was carried out for the period of 14–19 June 2023. The results are presented in Fig. 7 (W10), Fig. 8 (RH%), and Fig. 9 (2 m temperature).

During this period, tropical cyclone Biparjoy intensified into an Extremely Severe Cyclonic Storm (ESCS) over the Arabian Sea, where it persisted for nearly 10 days, which is a long lifetime for a pre-monsoon system. Its large cyclonic circulation (Fig. 7) drew substantial moisture from the Arabian Sea into the western Indian states of Gujarat and Rajasthan, resulting in enhanced rainfall activity over those regions. However, this strong westward moisture convergence had an indirect but significant effect on eastern and central India. On the eastern edge of Biparjoy, subsidence and suppressed convection were observed, leading to a progressive drying of the lower troposphere. Consequently, the RH values dropped below 40–50% (Fig. 8) across large parts of Uttar Pradesh, Bihar, Jharkhand, and Odisha. At the same time, the cyclone's prolonged activity delayed the normal eastward progression of the southwest monsoon, which typically advances into eastern India by mid-June. This combination of delayed monsoon onset, persistent subsidence, and reduced moisture availability created highly favorable conditions for the intensification and persistence of the June 2023 heatwave (Fig. 9). Simultaneously, the presence of an anomalous ridge over eastern India further amplified large-scale subsidence and enhanced surface radiative heating. This synoptic configuration led to T_{max} values in excess of 42–46 °C.

3.3 Mean error for Exp12 and Exp06 for the HW region

For verification, the mean error (ME) is a widely used diagnostic to quantify the systematic bias of model forecasts against observations. Since the ME represents the difference between forecasts and observations, it not only measures accuracy but also allows direct interpretation of model tendencies: positive ME values indicate overprediction (warm bias) of T_{max}, while negative ME values indicate underprediction (cold bias). A comparison of the ME values between Exp06 and Exp12 forecasts for the period of 14–19 June 2023 over the region affected by this event (Uttar Pradesh, Bihar, Jharkhand, and Odisha) is presented in Fig. 10. The ME values were calculated for all lead times (Days 1 to 5), but for brevity, we are presenting the results only for Day 1, 3, and 5 lead times.

For the Day-1 lead time (first column of Fig. 10), the Exp12 forecasts show a strong warm bias across Odisha and

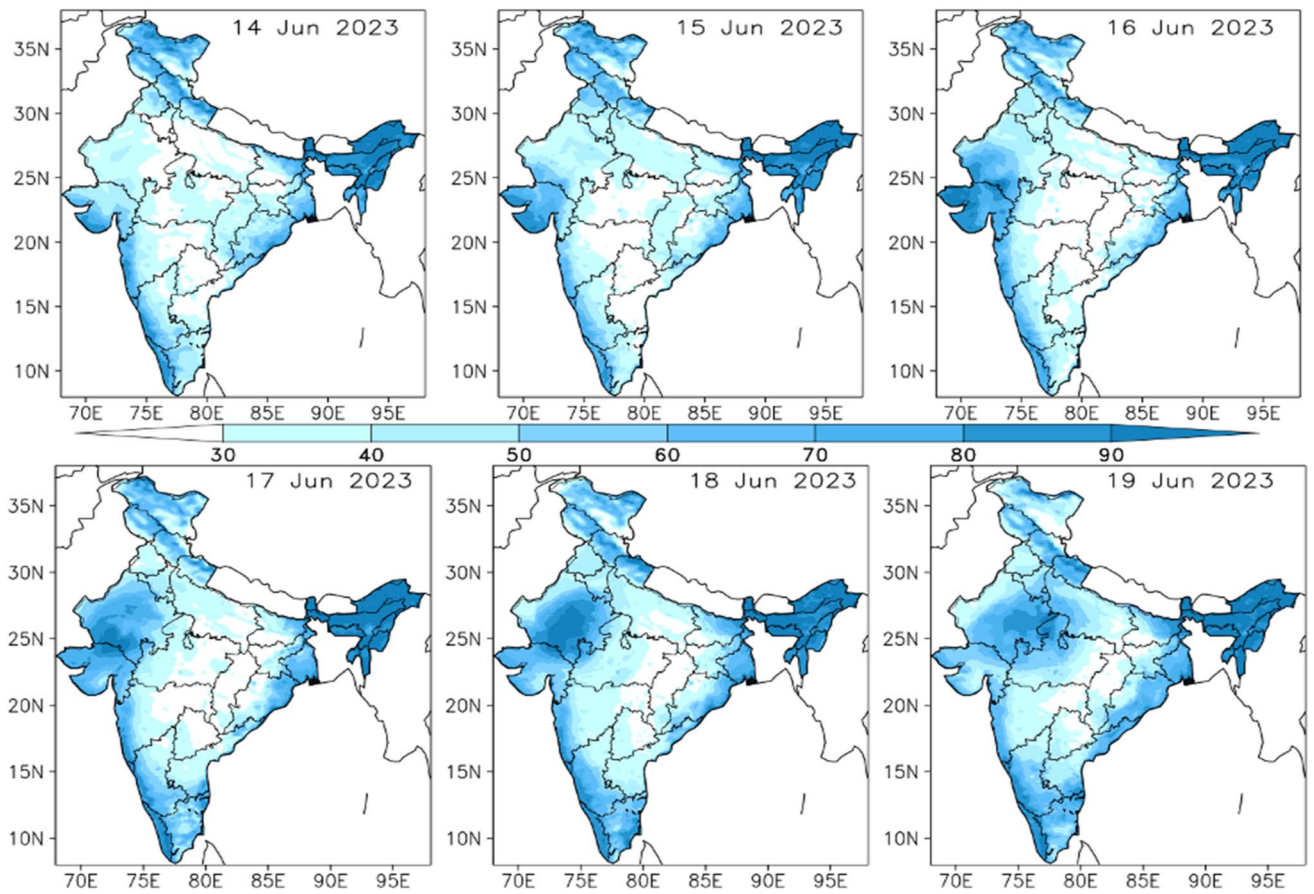

Fig. 8 Exp12 analysis 2 m RH (%) during 14–19 June 2023.

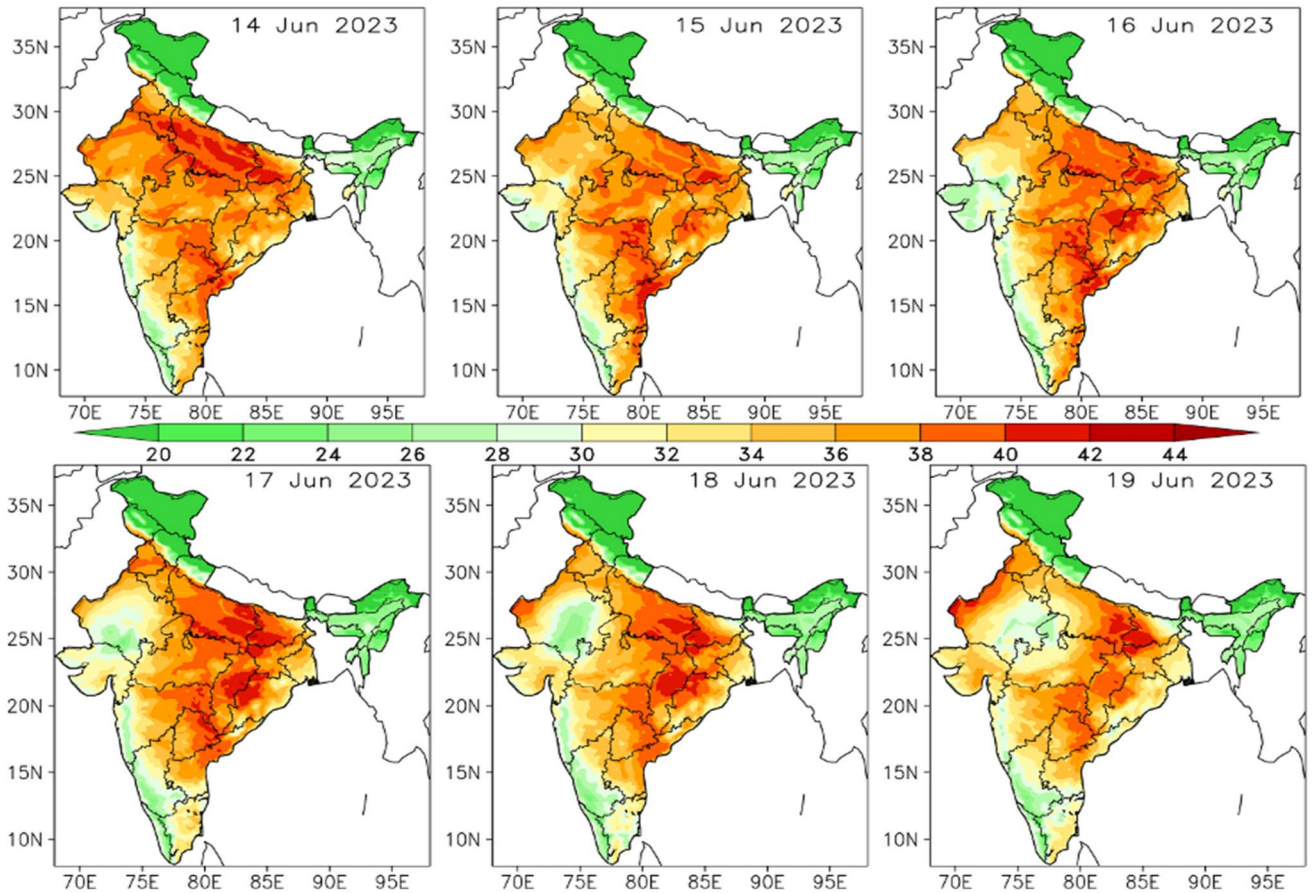

Fig. 9 Exp12 analysis 2 m Temperature during 14–19 June 2023.

Jharkhand, with ME values exceeding +3 to +5 °C, clearly indicating an overprediction of T_{max}. However, pockets of cold bias (negative ME, up to −2 °C) are evident in the eastern UP and parts of Bihar, indicating localized underestimation of T_{max}. In contrast, Exp06 demonstrates lower overall ME values, with warm biases confined mainly to coastal Odisha and smaller regions of Jharkhand, while cold biases remain weak and spatially limited. This suggests that Exp06 is better able to predict T_{max} and shows a reduction in both the magnitude and spatial extent of systematic errors in the short-range forecasts.

For Day 3 (second column of Fig. 10), Exp12 shows extensive warm biases across Odisha, Bihar, and Jharkhand (+3 to +4 °C), reflecting a systematic overestimation of T_{max}. At the same time, cold biases (−1 to −2 °C) are present over isolated regions of central India, pointing to regional underprediction of the temperature. Exp06 also produces warm biases at this lead time, although they are generally smaller in magnitude (+2 to +3 °C) with a more localized structure. Cold biases are seen more in Exp06 than Exp12, particularly over Jharkhand and Odisha, suggesting that the higher-resolution model may lead to the underprediction of T_{max}.

At the longer lead times of Day 5 (third column of Fig. 10), the magnitude of error for Exp06 is larger compared to that for Exp12. Over large parts of Odisha, Jharkhand, and West Bengal, Exp06 develops widespread warm biases, with ME values exceeding +5 °C. Cold biases are also evident (−2 to −3 °C) in some parts of Bihar and adjoining regions, highlighting the model's increasing spread in prediction error. Exp12, on the other hand, shows relatively smaller warm biases (generally +2 to +3 °C) and more spatially balanced error patterns, though it too retains some localized cold bias pockets. This indicates that while the performance of Exp06 is superior at short and medium ranges, its tendency to overpredict T_{max} intensifies at extended lead times, whereas Exp12 maintains more consistent error characteristics beyond Day 3.

3.4 Departure from climatology

Fig. 11 presents the departure of Day 1, 3, and 5 forecasts of T_{max} for both Exp12 and Exp06 from the observed climatology, along with their inter-model differences, for the period of 14–19 June 2023. The observations clearly indicate large positive departures of +4.5 °C to +6.5 °C for both versions, confirming the presence of widespread and intense heatwave conditions across eastern India.

For both Exp12 and Exp06, the forecasts capture the anomalously high T_{max} departures and reproduce the spatial extent of the heatwave well. Day 1 forecasts show strong positive departures over Odisha, Jharkhand, and adjoining Bihar, closely aligned with observations. For the Day 3 lead time, both models maintain the heatwave signal but tend to exaggerate the

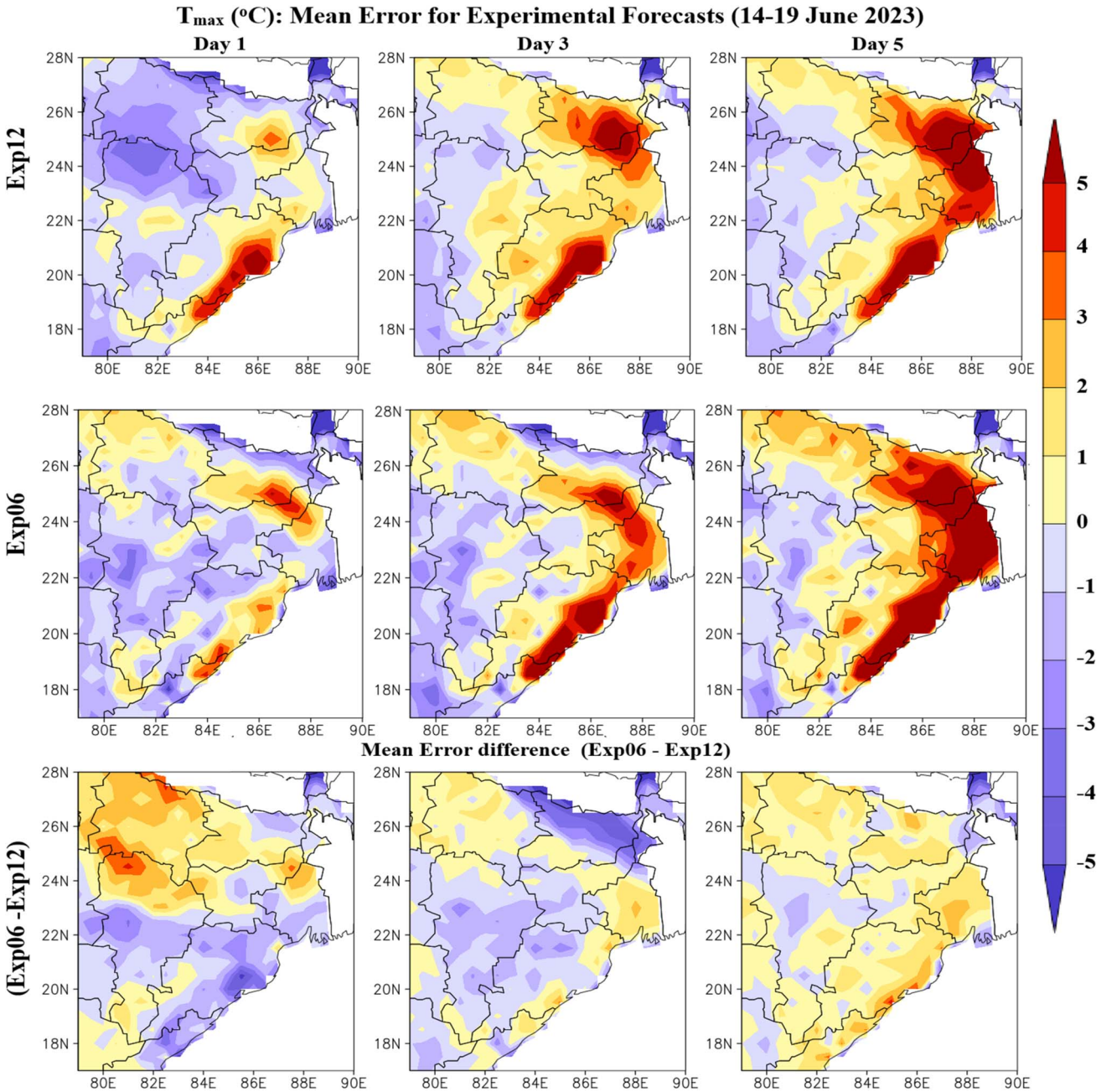

Fig. 10 Region-wise ME for Exp12 and Exp06 for the heatwave region.

magnitude of positive anomalies, particularly over northern Odisha, Jharkhand, and Bihar. For Day 5, the warm anomalies intensify further in both experiments, with Exp06 showing slightly larger departures than Exp12, particularly over Odisha and Bihar. This is consistent with the previous discussion about the ME, as the Exp06 exhibited larger errors for longer lead times.

The difference plots (Exp06–Exp12) show these tendencies more clearly. For the Day 1 lead time, the two models are nearly identical, with negligible differences. By Day 3, Exp06 produces warmer departures (by ~1–3 °C) across Jharkhand, Bihar, and eastern UP compared to the results for Exp12, suggesting a tendency for stronger amplification of the heatwave signal. This difference persists on Day 5, where Exp06 remains consistently warmer than Exp12 across the core heatwave belt, with localized differences exceeding +3 °C.

Overall, the analysis demonstrates that both models successfully captured the anomalous heatwave conditions of June 2023, but Exp06 systematically produced stronger positive departures at longer lead times, indicating a tendency to over-intensify heat extremes compared to the results for Exp12, which can lead to increased false alarms. While the underlying physics is unchanged, the high resolution reduces spatial averaging and permits a sharper representation of surface heterogeneity and gradients.[33] This often enhances the intensity of simulated anomalies, leading to a tendency for

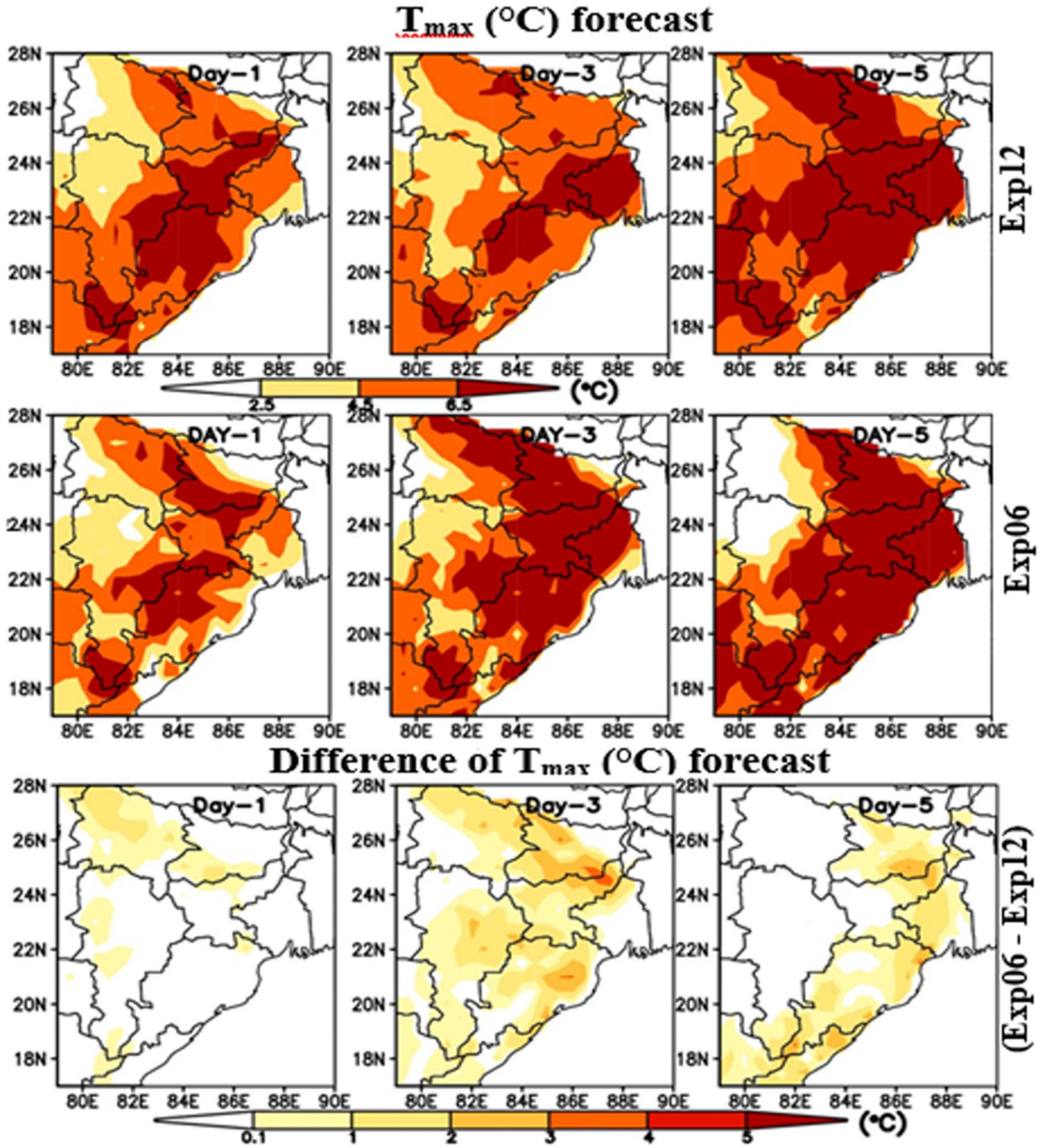

Fig. 11 Departure of the Day 1, 3 and 5 experimental T_{max} forecasts from the climatological values (upper and middle panel), and the differences in the departures (lower panel), valid for 14–19 June 2023.

overprediction; nonetheless, the high resolution remains critical for capturing localized extremes, such as heatwaves.

3.5 Region-based verification

To assess whether the increased horizontal resolution improves the ability of the model to represent the intensity and

Table 4 Regional information of various heat wave regions for 14–19 June 2023

Region name	Longitude	Latitude
Overall heat wave region (UPBOJ)	80°E–86°E	19°N–28°N
Uttar Pradesh and Bihar (UPB)	80°E–86°E	24°N–28°N
Odisha and Jharkhand (ODJ)	80°E–85°E	19°N–23°N

persistence of heatwaves, a region-wise verification was performed for three domains (Table 4): the combined heatwave core zone (UPBOJ), Uttar Pradesh and Bihar (UPB), and Odisha and Jharkhand (ODJ). Fig. 12 presents the time series of the observed, climatological, and forecasted T_{max} values from Exp12 and Exp06 for lead times of Day 1, Day 3, and Day 5 during 14–19 June 2023.

The climatological T_{max} for the UPBOJ region (first row of Fig. 12) is ~37 °C, whereas observations consistently show ~41–42 °C during the study period, indicating the intensity of the ongoing heatwave. Both models underestimate T_{max}, but Exp06 captures the anomalies more realistically. For Day 1, Exp06 simulates ~40–41 °C, reducing the cold bias relative to the results of Exp12, which is closer to the climatological value (~38–39 °C). At longer lead times (Day 5), Exp06 continues to track observations closely, maintaining the observed rising tendency, whereas Exp12 lags by 2–3 °C. This demonstrates that Exp06 not only better represents the departure from climatology but also sustains the heatwave intensity over extended lead times.

The UPB region (second row of Fig. 12) exhibits the most pronounced heat extremes, with the observed T_{max} reaching 42–43 °C. In this area, Exp12 systematically under-predicts the temperatures, with forecasts remaining closer to the climatological baseline (~38 °C) for Day 1 and Day 3. Exp06, however, demonstrates a clear advantage, reproducing the higher observed values and capturing day-to-day variability. For the Day 5 lead time, Exp06 retains the temperature agreement with the observations, reducing the systematic underestimation seen for Exp12. This indicates that Exp06 is better able to capture the regional amplification of heatwaves over the Indo-Gangetic plains.

Out of the three regions, for the relatively more humid ODJ region (third row of Fig. 12), the observed T_{max} remains around

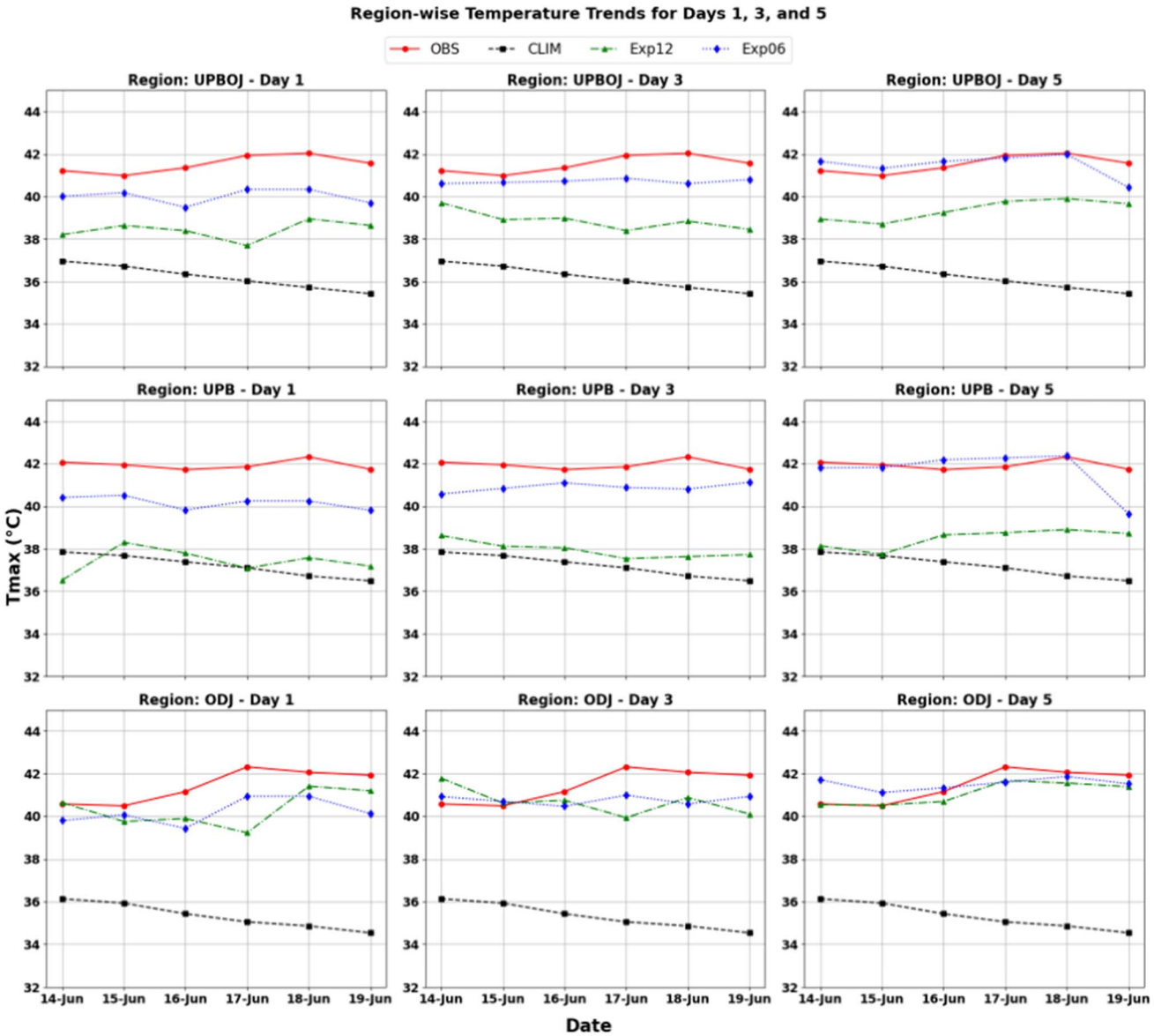

Fig. 12 Regional verification of T_{max} for Exp06 and Exp12 while comparing with the climatological and observation values.

~41 °C, compared to the climatological baseline of ~36 °C. For Day 1 and Day 3 lead times, both models underestimate the magnitude of warming but follow the observed temporal variability well. Between 14 and 16 June, the forecasts from both Exp12 and Exp06 align closely with observations, but from 17 to 19 June, both models exhibit a cold bias. Nevertheless, Exp06 tends to predict marginally higher temperatures than Exp12, thereby reducing the overall departure from observations. By Day 5, forecasts from both models converge towards the observed values, indicating a better representation of sustained heatwave intensity at longer lead times.

This regional verification shows that, on average, Exp06 consistently outperforms Exp12 in reproducing both the intensity and persistence of heatwaves, particularly over the drier areas (UPB and the combined UPBOJ region). The higher-resolution forecasts reduce the cold bias evident in Exp12 and better capture the day-to-day evolution of T_{max} anomalies, especially at long lead times. In contrast, over more humid regions such as ODJ, both models perform comparably, suggesting that resolution alone is insufficient and additional improvements in physics may be needed to further constrain biases. Overall, the results establish Exp06 as a more reliable system for operational heatwave monitoring, especially when accurate early warning is critical for societal preparedness.

3.6 *T*-test for determining the statistical significance of the improvement in ME

To quantitatively evaluate whether the differences between Exp06 and Exp12 are statistically meaningful, a paired *t*-test was performed on the average ME values aggregated across all lead times (Day 1–5) for each region. This choice was made to increase the effective sample size and provide a more robust estimate of the model performance differences, rather than relying on individual days where variability might mask systematic behavior. The results are presented in Table 5.

These results indicate that over UPBOJ (combined region), Exp06 exhibits improvement that is statistically significant at the 90% level, indicating moderate confidence in the increased resolution. For the UPB region, the Exp06 forecasts show statistically significant improvement at the 95% confidence level, demonstrating that higher resolutions provide a clear advantage in capturing heatwave intensity in this subregion. However, over the ODJ region, the differences between Exp06 and Exp12 are not statistically significant, suggesting that regional factors, such as land–surface processes or synoptic-scale circulation, may dominate over resolution effects.

Table 5 Paired *t*-test results for the improvements in the ME values between Exp12 and Exp06 with significance levels

Region	*t*-Statistic	*p*-Value	Significant at 95%	Significant at 90%
UPBOJ	−2.2133	0.0913	FALSE	TRUE
UPB	−3.5497	0.0238	TRUE	TRUE
ODJ	−1.0813	0.3404	FALSE	FALSE

The *t*-test results confirm that the benefits of a high resolution are region and lead-time-dependent. While Exp06 improves forecasts in areas with the most intense heatwave anomalies (*e.g.*, UPB), its advantages are less pronounced in other areas. These results emphasize the importance of operational adoption of high-resolution models for short-range decision-making during extreme heat events while highlighting the need for additional methods, such as statistical bias correction and ensemble post-processing, to improve reliability across regions and lead times.

4. Summary and conclusions

The number and intensity of heatwaves over India have seen a significant increase over the past decades, and therefore, it is of utmost importance to have NWP models that are able to accurately predict the occurrence and intensity of these events. At NCMRWF, a high-resolution (6 km) global NWP model was developed and run on an experimental basis. This study evaluated the performance of the NCUM-G at two horizontal resolutions: 12 km (Exp12) and 6 km (Exp06), to simulate the severe heatwave over eastern India during 14–19 June 2023. Both experiments were initialized with identical Hybrid 4D-Var analyses and employed the same physics, enabling isolation of the impact of horizontal resolution on the maximum temperature (T_{max}) forecasts. Some salient conclusions drawn based on the analysis in this study are listed below:

- Long-term analysis (1979–2022) showed a marked increase in the frequency of extremely hot days (>40 °C, >43 °C, >45 °C), particularly in the past two decades. In June 2023, the heatwave core shifted anomalously eastward into Uttar Pradesh, Bihar, Jharkhand, and Odisha, with T_{max} anomalies of +4.5–6.5 °C above climatology, fulfilling IMD's criteria for severe heatwaves.
- The prolonged lifetime of ESCS Biparjoy drew moisture westward into Gujarat and Rajasthan, delaying the advance of the southwest monsoon over eastern India. At the same time, subsidence and ridge formation over the eastern region enhanced surface heating and suppressed convection, sustaining daily T_{max} values of 42–46 °C for nearly a week.
- Forecast verification indicates that Exp06 exhibited lower ME values at short lead times (Day 1 and Day 3), reducing the cold biases evident in Exp12, particularly over Uttar Pradesh and Bihar. At longer ranges (Day 5), Exp12 produced more consistent forecasts, while Exp06 showed a tendency to over-predict T_{max}.
- Climatological departures show that both models captured the magnitude and spatial extent of positive anomalies, but Exp06 systematically produced stronger warm departures beyond Day 3.
- Regional verifications show that over the UPB and UPBOJ domains, Exp06 closely matched the observed T_{max} evolution, particularly on Day 5, while Exp12 forecasts remained closer to the climatological values. Over the more humid ODJ region, both models performed comparably. Similar findings were also obtained in previous studies over Bangladesh, where high moisture availability was observed.[34,35]

• Statistical testing was conducted, and paired *t*-tests of the average ME across all lead times confirmed that Exp06's improvement was statistically significant at the 95% level for the UPB region and at the 90% level for the combined UPBOJ region. No significant improvement was found over ODJ, indicating the region-dependent benefits of enhanced resolution.

It can be concluded from the study that Exp06 demonstrates clear advantages for short-range heatwave prediction in eastern India, particularly over drier subregions where small-scale land–atmosphere processes are critical. However, it has a tendency to amplify anomalies at longer lead times.

This study shows both the benefits and limitations of high-resolution global forecasts for heatwaves. Currently, work is going on at NCMRWF to expand the evaluation to multiple seasons, applying process-based diagnostics and integrating high-resolution runs into ensembles to balance accuracy across lead times. Furthermore, bias correction and post-processing are being carried out on the model forecasts, which are required for reducing systematic errors. Overall, high-resolution models improve confidence in early warnings but are most effective when combined with ensembles, calibration methods, and long-term validation.

Author contributions

SS was involved in conceptualization methodology, software, validation, formal analysis, investigation, resources, writing – original draft, and visualization. HS was involved in data curation, methodology, software, formal analysis, validation, and visualization. MNRS was involved in model run. AC, AD, RA, and VP contributed to conceptualization, investigation, writing—review, editing, and supervision.

Conflicts of interest

The authors declare no conflict of interest associated with this study.

Data availability

The analysis codes and data can be provided on request.

Acknowledgements

Sakshi Sharma acknowledges NCMRWF for providing access to HPC MIHIR for conducting the numerical experiments. We are grateful to IIT Kharagpur for the help and support. The scientific discussions with the renowned scientists of NCMRWF are greatly acknowledged. We are grateful to the anonymous reviewers for their constructive comments and suggestions that helped to improve the standard of the manuscript.

References

1 V. Masson-Delmotte, P. Zhai, A. Pirani, S. L. Connors, C. Péan, S. Berger, N. Caud, Y. Chen, L. Goldfarb, M. I. Gomis, *Climate change 2021: the physical science basis*, Contribution of working group I to the sixth assessment report of the intergovernmental panel on climate change, 2021, 2, pp. 1–2391.
2 *Climate Change 2001: Impacts, Adaptation, and Vulnerability: Contribution of Working Group II to the Third Assessment Report of the Intergovernmental Panel on Climate Change*, ed. J. J. McCarthy, Cambridge university press, 2001.
3 R. Akhtar, *Climate Change and Health and Heat Wave Mortality in India*, 2007.
4 *Managing the Risks of Extreme Events and Disasters to Advance Climate Change Adaptation: Special Report of the Intergovernmental Panel on Climate Change*, C. B. Field, Cambridge University Press, 2012.
5 *Climate Change 2013: the Physical Science Basis: Working Group I Contribution to the Fifth Assessment Report of the Intergovernmental Panel on Climate Change*, ed. T. Stocker, Cambridge university press, 2014.
6 G. Basha, P. Kishore, M. V. Ratnam, A. Jayaraman, A. Agha Kouchak, T. B. Ouarda and I. Velicogna, Historical and projected surface temperature over India during the 20th and 21st century, *Sci. Rep.*, 2017, 7(1), 2987.
7 D. S. Pai, S. Nair and A. N. Ramanathan, Long term climatology and trends of heat waves over India during the recent 50 years (1961-2010), *Mausam*, 2013, **64**(4), 585–604.
8 P. Rohini, M. Rajeevan and A. K. Srivastava, On the variability and increasing trends of heat waves over India, *Sci. Rep.*, 2016, **6**(1), 1–9.
9 A. K. Jaswal, P. C. Rao and V. Singh, Climatology and trends of summer high temperature days in India during 1969–2013, *J. Earth Syst. Sci.*, 2015, **124**(1), 1–5.
10 K. Ray, R. K. Giri, S. S. Ray, A. P. Dimri and M. Rajeevan, An assessment of long-term changes in mortalities due to extreme weather events in India: A study of 50 years' data, 1970–2019, *Weather Clim. Extrem.*, 2021, **32**, 100315.
11 P. Kumar, A. Rai, A. Upadhyaya and A. Chakraborty, Analysis of heat stress and heat wave in the four metropolitan cities of India in recent period, *Sci. Total Environ.*, 2022, **818**, 151788.
12 U. S. De, R. K. Dube and G. P. Rao, Extreme weather events over India in the last 100 years, *J Indian Geophys Uni.*, 2005, **9**(3), 173–187.
13 A. K. Srivastava, M. Rajeevan and S. R. Kshirsagar, Development of a high resolution daily gridded temperature data set (1969–2005) for the Indian region, *Atmos. Sci. Lett.*, 2009, **10**(4), 249–254.
14 S. K. Chaudhury, J. M. Gore and K. S. Ray, Impact of heat waves over India, *Curr. Sci.*, 2000, **79**(2), 153–155.
15 J. V. Ratnam, S. K. Behera, S. B. Ratna, M. Rajeevan and T. Yamagata, Anatomy of Indian heatwaves, *Sci. Rep.*, 2016, **6**(1), 1.
16 T. Clima, and W. Te, Guidelines on the Definition and Characterization of Extreme Weather and Climate Events, 2023, pp. 2–16.
17 IMD, *Standard Definitions of Meteorological Terms. India Meteorological Department, Ministry of Earth Sciences*, Government of India, 2016, available from: **https://internal.imd.gov.in/section/nhac/dynamic/FAQ_heat_wave.pdf**.

18 National Oceanic and Atmospheric Administration/National Weather Service, *The Heat Index Equation (Stedman's Apparent Temperature)*, NOAA, Washington, DC, 2011, **https://www.wpc.ncep.noaa.gov/html/heatindex_equation.shtml**.

19 *Heatwaves and Health: Guidance on Warning-System Development*, ed. G. R. McGregor, P. Bessemoulin, K. L. Ebi, and B. Menne, World Meteorological Organization, Geneva, Switzerland, 2015.

20 J. C. Montero, I. J. Miron, J. J. Criado, C. Linares and J. Díaz, Difficulties of defining the term,"heat wave", *Int. J. Environ. Health Res.*, 2013, **23**(5), 377–379.

21 G. S. Azhar, D. Mavalankar, A. Nori-Sarma, A. Rajiva, P. Dutta, A. Jaiswal, P. Sheffield, K. Knowlton and J. J. Hess, Heat-related mortality in India: excess all-cause mortality associated with the 2010 Ahmedabad heat wave, *PLoS One*, 2014, **9**(3), e91831.

22 H. Singh, A. Dube, S. Kumar and R. Ashrit, Bias correction of maximum temperature forecasts over India during March–May 2017, *J. Earth Syst. Sci.*, 2020, **129**(1), 13.

23 A. Dube, H. Singh and R. Ashrit, Heat waves in India during MAM 2019: Verification of ensemble based probabilistic forecasts and impact of bias correction, *Atmos. Res.*, 2021, **251**, 105421.

24 K. C. Gouda, S. K. Sahoo, P. Samantray and S. Himesh, Simulation of extreme temperature over Odisha during May 2015, *Weather Clim. Extrem.*, 2017, **17**, 17–28.

25 V. Mishra, S. Mukherjee, R. Kumar and D. A. Stone, Heat wave exposure in India in current, 1.5 C, and 2.0 C worlds, *Environ. Res. Lett.*, 2017, **12**(12), 124012.

26 E. N. Rajagopal, G. R. Iyengar, J. P. George, M. D. Gupta, S. Mohandas, R. Siddharth, A. Gupta, M. Chourasia, V. S. Prasad, K. S. Aditi, and A. Ashish, *Implementation of Unified Model Based Analysis-Forecast System at NCMRWF*, InInternal Report, NMRF/TR/2/2012, National Centre for Medium Range Weather Forecasting, India, 2012, pp. 1–45, Ministry of Earth Sciences.

27 J. P. George, S. I. Rani, A. Jayakumar, S. Mohandas, S. Mallick, A. Lodh, R. Rakhi, M. N. Sreevathsa, and E. N. Rajagopal, NCUM data assimilation system, *National Centre for Medium Range Weather Forecasting*, 2016.

28 S. Kumar, R. S. Indira, J. P. George and E. N. Rajagopal, Megha-tropiques SAPHIR radiances in a hybrid 4D-Var data assimilation system: Study of forecast impact, *Q. J. R. Metereol. Soc.*, 2018, **144**(712), 792–80528.

29 R. Ashrit, S. Indira Rani, S. Kumar, S. Karunasagar, T. Arulalan, T. Francis, A. Routray, S. I. Laskar, S. Mahmood, P. Jermey and A. Maycock, IMDAA regional reanalysis: performance evaluation during Indian summer monsoon season, *J. Geophys. Res.:Atmos.*, 2020, **125**(2), e2019JD030973.

30 J. Caesar, L. Alexander and R. Vose, Large-scale changes in observed daily maximum and minimum temperatures: Creation and analysis of a new gridded data set, *J. Geophys. Res.:Atmos.*, 2006, **111**(D5), 1–10.

31 F. Rawlins, S. P. Ballard, K. J. Bovis, A. M. Clayton, D. Li, G. W. Inverarity, A. C. Lorenc and T. J. Payne, The Met Office global four-dimensional variational data assimilation scheme, *Q. J. R. Meteorol. Soc.*, 2007, **133**(623), 347–362.

32 D. Walters, A. J. Baran, I. Boutle, M. Brooks, P. Earnshaw, J. Edwards, K. Furtado, P. Hill, A. Lock, J. Manners and C. Morcrette, The Met Office Unified Model global atmosphere 7.0/7.1 and JULES global land 7.0 configurations, *Geosci. Model Dev.*, 2019, **12**(5), 1909–1963.

33 M. L. Weisman, W. C. Skamarock and J. B. Klemp, The resolution dependence of explicitly modeled convective systems, *Mon. Weather Rev.*, 1997, **125**(4), 527–548.

34 M. M. Rahman, M. A. Mannan, M. S. Sarkar, M. A. Mallik, A. Sultana, M. K. Islam, M. Y. Akter, E. Alam and A. R. Islam, Are hotspots and frequencies of heat waves changing over time? Exploring causes of heat waves in a tropical country, *PLoS One*, 2024, **19**(5), e0300070.

35 M. B. Rahman, R. Salam, A. R. Islam, A. Tasnuva, U. Haque, S. Shahid, Z. Hu and J. Mallick, Appraising the historical and projected spatiotemporal changes in the heat index in Bangladesh, *Theor. Appl. Climatol.*, 2021, **146**(1–2), 125.